

LA-UR- 91 - 589

CONF-70

LA-UR--91-589

DE91 008593

Los Alamos National Laboratory is operated by the University of California for the United States Department of Energy under contract W-7405-ENG-36

TITLE LAYER TRACKING ASYMPTOTICS AND DOMAIN DECOMPOSITION

AUTHOR(S) David L. Brown  
R. C. Y. Chin  
G. W. Hedstrom  
T. A. Mantauffel

SUBMITTED TO Proceedings for the ICASE Workshop on  
Heterogeneous Boundary Condition

### DISCLAIMER

This report was prepared as an account of work sponsored by an agency of the United States Government. Neither the United States Government nor any agency thereof, nor any of their employees, makes any warranty, express or implied, or assumes any legal liability or responsibility for the accuracy, completeness, or usefulness of any information, apparatus, product, or process disclosed, or represents that its use would not infringe privately owned rights. Reference herein to any specific commercial product, process, or service by trade name, trademark, manufacturer, or otherwise does not necessarily constitute or imply its endorsement, recommendation, or favoring by the United States Government or any agency thereof. The views and opinions of authors expressed herein do not necessarily state or reflect those of the United States Government or any agency thereof.

By accepting this notice, the publisher acknowledges that this is a government report, is not subject to copyright, and is free to use in publishing or reproducing this report for any purpose, without charge, for the purpose of providing information to the public.

This report is available to the public through the National Technical Information Service, Springfield, Virginia 22161.

Los Alamos Los Alamos National Laboratory  
Los Alamos, New Mexico 87545

# **Layer tracking, asymptotics, and domain decomposition**

David L. Brown, Computing and Communications Div., LANL, Los Alamos, NM 87545

R. C. Y. Chin, Computer Science, IUPUI, Indianapolis, IN 46205

G. W. Hedstrom, LLNL, L-321, P. O. Box 808, Livermore, CA 94550

T. A. Manteuffel, University of Colorado Denver, Denver, CO 80202

## **Abstract**

In this paper we present a preliminary report on our work on the tracking of internal layers in a singularly-perturbed convection-diffusion equation. We show why such tracking may be desirable, and we also show how to do it using domain decomposition based on asymptotic analysis.

## 1. Introduction.

In this paper we present the analogue of a shock-tracking scheme for the resolution of an internal layer and its interaction with an ordinary boundary layer at the outflow. In the computation of compressible flows at high Mach number there has long been competition between shock tracking and shock capturing, and it is now generally agreed that both are needed. We generally find that the number of strong shocks is small, and they should be tracked in order to assure accuracy of the solution. For reasons of efficiency, however, the large number of weak shocks reverberating around the domain should be computed by a reliable shock-capturing scheme such as Roe's method [14] or the method of Colella and Woodward [7]. Shocks are not always the most important features in fluid flows, but the tracking of such other phenomena is still far behind shock tracking. We first show why it may be desirable to track an internal layer, and then we show how such tracking may be accomplished via domain decomposition.

For the sake of simplicity we consider a specific time-independent, singularly-perturbed, convection-diffusion equation

$$a \partial_x u + b \partial_y u = \epsilon \Delta u + F \quad (1.1)$$

on a bounded domain  $\Omega$  in the  $(x, y)$ -plane. Here,  $\Delta$  denotes the Laplace operator, and  $\epsilon$  is a small, positive number. For the moment, we impose Dirichlet conditions  $u = f$  on the boundary  $\partial\Omega$ , but later we sometimes treat mixed boundary conditions. The function  $f$  is required to be piecewise smooth. (We use the term 'smooth' to mean some convenient degree of differentiability, say  $C^2$ .) We assume that the coefficients  $a$  and  $b$  are smooth functions of  $x$  and  $y$  on  $\Omega$ . The source term  $F$  is assumed to be a smooth function of  $x$ ,  $y$ , and  $u$ . Furthermore, we impose the restriction that  $|a| + |b| \neq 0$  in the closure of  $\Omega$ . This assumption implies that there are no stagnation points, and it greatly diminishes the complexity of the domain decomposition. Our assumption of semilinearity is much less restrictive because nonlinear problems are often solved via a sequence of linear problems with variable coefficients. Our discussion does not pertain to shock layers, however, since they violate the assumption of smoothness of  $a$  and  $b$ .

Previous work, [4], [11], [12] on algorithms for (1.1) using domain decomposition based on asymptotic analysis has treated the special case of  $b = 0$ . It is true that a transformation of coordinates may be used to convert (1.1) to the case  $b = 0$ . In this paper we show why such a transformation is very desirable, and we present an algorithm to carry it out.

The development of numerical methods for (1.1) in the singularly perturbed case requires an understanding of the asymptotic behavior of its solutions as  $\epsilon \downarrow 0$ . We therefore begin with a brief description of the relationship between  $u$  and the solution

$U$  of the reduced equation

$$a \partial_x U + b \partial_y U = F. \quad (1.2)$$

For more details see the books by Chang and Howes [1] and Eckhaus [8]. Equation (1.2) is easily solved by the method of characteristics,

$$\frac{dx}{ds} = a, \quad \frac{dy}{ds} = b, \quad \frac{dU}{ds} = F. \quad (1.3)$$

The first two equations (1.3) define characteristic curves. It is clear that we cannot impose the boundary condition  $U = f$  at every intersection of a characteristic curve with  $\partial\Omega$ . Instead, we subdivide  $\partial\Omega$  into three sets, depending on the direction of the vector  $(a, b)$ . The *inflow boundary*  $\Gamma_I$  is the subset of  $\partial\Omega$  on which  $(a, b)$  points into  $\Omega$ , the *outflow boundary*  $\Gamma_O$  is the subset of  $\partial\Omega$  on which  $(a, b)$  points out of  $\Omega$ , and the *tangential boundary*  $\Gamma_T$  is the subset of  $\partial\Omega$  on which  $(a, b)$  is tangent to  $\partial\Omega$ . For (1.3) the boundary condition  $U = f$  is imposed only on the inflow boundary  $\Gamma_I$ .

It is reasonable to expect to have  $u \approx U$  for the solutions  $u$  of (1.1) wherever  $\Delta u$  is not too large, i.e., wherever  $u$  is smooth. Because of the smoothness of the source term  $F$  and of the coefficients  $a$  and  $b$ , the only mechanism for introducing nonsmooth behavior into the solution  $u$  of (1.1) is through the boundary condition  $u = f$ . One obvious difficulty is that we cannot force  $U = f$  on the outflow and tangential boundaries  $\Gamma_O \cup \Gamma_T$ . The resolution of this difficulty is that there are boundary layers across which  $u$  changes rapidly from  $u \approx U$  to  $u = f$ . More precisely, when  $f$  is smooth the relation  $u \approx U$  is true except in the following portions of  $\Omega$ . There may be what are called *parabolic boundary layers* along the tangential boundary  $\Gamma_T$ , and there may be *ordinary boundary layers* along the outflow boundary  $\Gamma_O$ .

Let us take a moment to explain the terminology 'ordinary boundary layer' and to describe its properties. Consider a point  $P$  on  $\Gamma_O$ . In the vicinity of  $P$  we may construct a transformation  $(\sigma, \tau) \mapsto (x, y)$  such that the origin  $(\sigma, \tau) = (0, 0)$  is mapped to the point  $P$ . We may further require that the portion of a neighborhood of the origin with  $\tau > 0$  is mapped into  $\Omega$ , so that a segment of the axis  $\sigma = 0$  is mapped onto a segment of the boundary  $\Gamma_O$ . In terms of the variables  $\sigma$  and  $\tau$  the differential equation (1.1) takes the form

$$\hat{a} \partial_\sigma u + \hat{b} \partial_\tau u = \epsilon (c_1 \partial_\sigma^2 u + c_2 \partial_\sigma \partial_\tau u + c_3 \partial_\tau^2 u) + F. \quad (1.4)$$

Note that the definition of outflow boundary implies that if  $c_1$  is chosen to be positive, then it follows that  $\hat{a} < 0$ . We have seen that we expect to have  $u \approx U$  away from the boundary  $\sigma = 0$ , while we require that  $u = f$  on the boundary  $\sigma = 0$ . That is, we expect  $u$  to vary slowly with respect to  $\tau$  but rapidly with respect to  $\sigma$ . Let us therefore introduce the scaling

$$\sigma = \epsilon \sigma', \quad \tau = \tau' \quad (1.5)$$

into (1.4). If we formally discard all but terms of the order of  $1/\epsilon$ , we obtain a reduced equation

$$\hat{a} \partial_{\hat{\sigma}} V = c_1 \partial_{\hat{\sigma}}^2 V. \quad (1.6)$$

The term ordinary boundary layer derives from the fact that (1.6) is an ordinary differential equation. The term exponential boundary layer is also used, because the solution  $V$  of (1.6) is the sum of a constant and an exponential function. Note that because  $\hat{a}/c_1 < 0$ , this exponential decreases with increasing  $\hat{\sigma}$ . Note also that in terms of the variable  $\sigma$  the rate of decrease is of the order of  $\exp\{-\kappa\sigma/\epsilon\}$ , where  $\kappa$  is an average value of  $|\hat{a}|/c_1$ . We therefore expect the width of the ordinary boundary layer to be  $O(\epsilon)$ . The book by Chang and Howes [1] gives theoretical justification for all of these heuristic manipulations.

In the vicinity of the tangential boundary  $\Gamma_T$  we use the characteristic curves (1.3) to define one set of coordinate lines, and we use them as the foundation for a local mapping  $(s, t) \mapsto (x, y)$  in the vicinity of a point  $P$  on  $\Gamma_T$ . In terms of these coordinates (1.1) takes the form

$$\partial_s u = \epsilon(c_4 \partial_s^2 u + c_5 \partial_s \partial_t u + c_6 \partial_t^2 u) + F. \quad (1.7)$$

We remark that the definition of flow direction implies that  $c_6 > 0$ . We may require that a segment of the axis  $t = 0$  maps onto a segment of the boundary  $\Gamma_T$  and that positive values of  $t$  correspond to points in the interior of  $\Omega$ . Thus, the boundary layer has to accommodate a rapid transition from  $u \approx U$  for  $t > 0$  to  $u = f$  at  $t = 0$ . Let us therefore introduce the scaling

$$s = \hat{s}, \quad t = \hat{t}\sqrt{\epsilon} \quad (1.8)$$

into (1.7). If we formally delete all terms smaller than  $O(1)$ , we obtain the reduced equation

$$\partial_{\hat{s}} W = c_4 \partial_{\hat{t}}^2 W + F. \quad (1.9)$$

This equation is parabolic, giving rise to the term parabolic boundary layer. Furthermore, the thickness of the boundary layer for (1.9) is  $O(1)$  with respect to  $\hat{t}$ . With respect to  $t$  the parabolic boundary layer is therefore of width  $O(\sqrt{\epsilon})$ . Again, theoretical justification for these remarks may be found in [1].

If  $f$  has a discontinuity at a point  $P$  on  $\Gamma_T$ , then by (1.3) the function  $U$  will have a corresponding discontinuity in  $\Omega$  along the characteristic curve  $\gamma$  through  $P$ . Similarly, if the Lie derivative of  $f$  along  $\Gamma_T$  is discontinuous at  $P$ , then  $\text{grad } U$  is discontinuous along  $\gamma$ . Because  $u$  is smooth, the lack of smoothness of  $U$  causes  $u$  to deviate substantially from  $U$  in a neighborhood of  $\gamma$ . As in the case of a parabolic boundary layer, if we introduce coordinates  $(s, t)$  derived from the characteristic variable  $s$  as given by (1.3), we find that (1.1) maps to an equation of the form (1.7) and

that (1.9) is the appropriate reduced equation. We are therefore led to the conclusion that such an *internal layer* is parabolic in nature and that its width is  $O(\sqrt{\epsilon})$ . We again refer the reader to [1] for further justification.

In the next section we analyze the behavior of a standard central difference scheme when there is an internal layer tilted at an angle to the grid, and we show that numerical approximation introduces downstream oscillations unless the internal layer is resolved. Therefore we must use either a fine grid, an artificial increase of the viscosity  $\epsilon$ , or a grid aligned with the layer. Here we are discussing a grid effect, in that Hedstrom and Osterheld [13] showed that the numerical errors for a coarse grid aligned with an internal layer are minimal even at large cell Reynolds numbers.

In Section 3 we present an algorithm for the construction of an orthogonal grid with one coordinate direction aligned to the vector field  $(a, b)$ . This mapping requires the solution of the telegraphers' equation. In Section 4 we introduce a domain decomposition for a problem (1.1) with an internal layer and an ordinary boundary layer. In this domain decomposition the ordinary boundary layer and the internal layer have their own subdomains, and there is a separate subdomain for the region where these layers interact. In addition, in each subdomain a separate numerical method is used, depending on the local asymptotic behavior of the solution.

## 2. A layer tilted to the grid.

In this section we use a heuristic argument based on the modified equation to show why it is generally unwise to permit an internal layer not to be aligned with the grid. Specifically, we show that the standard central-difference scheme has grid directions which are modelled by a modified equation in the style of Warming and Hyett [9]. See Griffiths and Sanz-Serna [10] for a more modern exposition on modified equations. We shall see that the solutions of the modified equation are integrals of Airy functions, multiplied by a decaying exponential. The oscillations of this Airy function may or may not be damped by the exponential, depending on the values of a dimensionless parameter. We also derive the modified equation for the upwind difference scheme, and as may be expected, we find that upwinding adds numerical diffusion.

For the discussion here we restrict our attention to the special case when the coefficients  $a$  and  $b$  in (1.1) are constant and the source term  $F$  vanishes. Then for convection with velocity  $V$  in the direction  $(\cos \theta, \sin \theta)$  we have the convection-diffusion equation

$$V \cos \theta \partial_x u + V \sin \theta \partial_y u = \epsilon \Delta u.$$

The reduced equation for (2.1) is

$$V \cos \theta \partial_x U + V \sin \theta \partial_y U = 0, \quad (2.2)$$

and its characteristic curves are given by

$$\frac{dx}{ds} = V \cos \theta, \quad \frac{dy}{ds} = V \sin \theta. \quad (2.3)$$

For the discussion here it suffices to restrict our attention to directions  $0 \leq \theta \leq \pi/4$ . We remark that the special case  $\theta = 0$  of flow parallel to the grid was examined by Hedstrom and Osterheld [13].

For (2.1) we use a rectangular domain

$$\Omega = \{(x, y): 0 < x < 1, 0 < y < 1\}. \quad (2.4)$$

Thus, under the conditions that  $0 \leq \theta \leq \pi/4$  the inflow boundary is at  $x = 0$  and at  $y = 0$ , and the other two sides of the rectangle comprise the outflow boundary. On the inflow boundary we select a point of discontinuity  $y_0$ , and we impose the conditions

$$u = \begin{cases} 0.5(1 + \operatorname{sgn}(y - y_0)) & \text{for } x = 0, \\ 0 & \text{for } y = 0. \end{cases} \quad (2.5)$$

The discontinuity in the boundary data at  $y_0$  induces an internal layer along the characteristic curve  $x \sin \theta - (y - y_0) \cos \theta = 0$ . In fact, the solution  $U$  to the reduced equation (2.2) with boundary data (2.5) is given by

$$U = \frac{1}{2} - \frac{1}{2} \operatorname{sgn}(x \sin \theta - (y - y_0) \cos \theta). \quad (2.6)$$

In order to minimize ordinary boundary layers along the outflow boundary, we impose the reduced equation (2.2) as boundary condition at  $x = 1$  and at  $y = 1$ .

Consider the standard central-difference scheme for (2.1). We impose a square grid on  $\Omega$  with mesh size  $h$ , and we define the shift operators

$$T_x v(x, y) = v(x + h, y), \quad T_y v(x, y) = v(x, y + h). \quad (2.7)$$

With this notation the central-difference approximation to (2.1) is

$$\frac{V \cos \theta}{2h} (T_x - T_x^{-1})v + \frac{V \sin \theta}{2h} (T_y - T_y^{-1})v = \epsilon Dv, \quad (2.8)$$

where  $D$  denotes the discrete Laplacian

$$D = \frac{1}{h^2} (T_x + T_y + T_x^{-1} + T_y^{-1} - 4I).$$

On the inflow boundary  $\Gamma_I$  the boundary conditions for (2.8) are (2.5). On the outflow boundary  $\Gamma_O$  we use an upwind discretization of (2.2).

The modified equation for (2.8) is best written in terms of the rotated coordinate system aligned with the flow direction

$$\begin{aligned} s &= x \cos \theta + (y - y_0) \sin \theta, \\ t &= -x \sin \theta + (y - y_0) \cos \theta. \end{aligned} \quad (2.9)$$

We also introduce scalings of  $s$  and  $t$  in order to derive a modified equation in dimensionless form and to identify the pertinent parameters. It happens that for (2.1) or (2.8) on the halfplane  $x > 0$  there is no natural length scale in the direction of the flow (the  $s$ -direction). One may as well use a length scale  $L = 1$ . For the rectangular domain  $\Omega$  defined in (2.4) it is reasonable to take  $L$  to be the width of  $\Omega$  ( $L = 1$ ) or the width of  $\Omega$  in the  $s$ -direction ( $L = \sec \theta$ ). We shall see that the natural scalings for the modified equation corresponding to the central difference method (2.8) are

$$\begin{aligned} s &= L\sigma, \\ t &= \tau \left( \frac{L\epsilon}{V} \right)^{1/2}. \end{aligned} \quad (2.10)$$

Furthermore, the important dimensionless parameters for (2.8) are the cell Reynolds number

$$R_h = \frac{hV}{\epsilon} \quad (2.11)$$

and the degree of streamwise resolution

$$\gamma = \frac{h}{L}. \quad (2.12)$$



In terms of these parameters the modified equation for (2.8) is given by the following theorem.

**Theorem.** Suppose that  $0 \leq \theta \leq \pi/4$ . Suppose also that  $\gamma \ll 1$  and that  $\gamma \ll R_h \ll 1/\gamma$ . Then the modified equation for (2.8) is

$$\partial_\sigma v = \partial_\tau^2 v - \frac{\sin(4\theta)}{24} \gamma^{1/2} R_h^{3/2} \partial_\tau^3 v + \left( \frac{\gamma}{R_h} + \frac{\gamma R_h}{48} (3 + \cos(4\theta)) \right) \partial_\sigma^2 v. \quad (2.13)$$

**Remarks.** The restriction that  $\gamma = h/L \ll 1$  is reasonable for numerical computations, since we would want features in the streamwise direction to be resolved. The condition that  $\gamma \ll R_h \ll 1/\gamma$  is also ordinarily satisfied in computations. We have written the modified equation in the form (2.13) in order to provide uniformity as  $\sin(4\theta) \rightarrow 0$ . The grid-induced oscillations appear only when  $\sin(4\theta) \neq 0$  and when  $R_h$  is moderately large. (Remember that we require  $R_h \gamma \ll 1$ .) Under the condition that  $R_h \sin(4\theta)$  is bounded away from zero, the modified equation (2.13) takes the simpler form

$$\partial_\sigma v = \partial_\tau^2 v - \frac{\sin(4\theta)}{24} \gamma^{1/2} R_h^{3/2} \partial_\tau^3 v. \quad (2.14)$$

In (2.14) the parameter

$$\beta = \frac{\sin(4\theta)}{24} \gamma^{1/2} R_h^{3/2} \quad (2.15)$$

measures the importance of the grid-induced numerical dispersion relative to the physical diffusion, and no numerically induced oscillations will be observed if  $\beta$  is sufficiently small. For boundary data  $v = \text{sgn}(\tau)$  at  $\tau = 0$  the solution of (2.14) may be expressed in terms of the Airy function, as is shown by Chin and Hedstrom [3]. In fact, a Fourier transformation with respect to  $\tau$  shows that

$$v(\sigma, \tau) = \frac{1}{2} + \int_{-\infty}^{\infty} \frac{1}{i2\pi\omega} \exp \{ i\beta\sigma\omega^3 - \sigma\omega^2 + i\tau\omega \} d\omega. \quad (2.16)$$

The reference [3] also provides figures and tables of the integrals (2.16) for various values of  $\beta$ . The upshot is that whether or not there are oscillations depends on a parameter

$$\alpha = \frac{2\sigma^{1/3}}{(2\beta)^{2/3}}. \quad (2.17)$$

If  $\alpha > 2$ , the diffusion is dominant, and there are no oscillations. For  $\alpha < 2$ , however, there is a sequence of damped oscillations below the layer ( $\tau < 0$ ). Because  $\alpha$  is an increasing function of  $\sigma$ , as we proceed downwind  $\sigma$  increases and the diffusion eventually removes the oscillations.

Note with regard to the applicability of the modified equation that the internal layer is many grid cells wide and that the oscillations have wavelengths spanning many grid cells. This behavior makes the modified equation applicable, in that the

derivation of a modified equation is based on the assumption that the numerical solution is smooth relative to the grid. The user of modified equations must always keep in mind that they are utterly useless in predicting variations in the numerical solution on the scale of 2 or 3 grid sizes.

Finally, we also remark that the upwind difference scheme

$$V \frac{\cos \theta}{h} (I - T_x^{-1})u + V \frac{\sin \theta}{h} (I - T_y^{-1})u = \epsilon D u$$

with the scalings (2.10) has the modified equation

$$\partial_\sigma v = \alpha_1 \partial_\tau^2 v + \alpha_2 \partial_\sigma^2 v$$

with

$$\alpha_1 = 1 + \frac{R_h}{2\sqrt{2}} \sin(2\theta) \cos\left(\frac{\pi}{4} - \theta\right),$$

$$\alpha_2 = \frac{\gamma}{R_h} + \frac{\gamma R_h}{48} \left(3 + \cos(4\theta) + 24(\cos^3 \theta + \sin^3 \theta)\right).$$

The most significant numerical viscosity added by the grid effect is the deviation of  $\alpha_1$  from 1.

**Proof of the theorem.** The idea of the modified equation is to make an ansatz that the solution of the difference scheme is smooth enough to be represented by a small number of terms of its Taylor expansion and to use this expansion to identify a partial differential equation which approximates (2.8) more closely than the original equation (2.1) does.

Thus, we begin with the assumption that some smooth function  $v$  is a solution of (2.8). In this case the word 'smooth' is taken to mean that we may use Taylor approximations such as

$$T_x v = v + h \partial_x v + \frac{h^2}{2} \partial_x^2 v + \frac{h^3}{6} \partial_x^3 v + \frac{h^4}{24} \partial_x^4 v \quad (2.18)$$

for the terms in (2.8). That is, we choose to neglect terms in the Taylor series approximation to (2.8) of order  $h^5$  and higher. We therefore obtain the equation

$$V \cos \theta \left( \partial_x v + \frac{h^2}{6} \partial_x^3 v \right) + V \sin \theta \left( \partial_y v + \frac{h^2}{6} \partial_y^3 v \right) \\ = \epsilon \left( \partial_x^2 v + \partial_y^2 v + \frac{h^2}{12} (\partial_x^4 v + \partial_y^4 v) \right).$$

The rotation of coordinates (2.9) then gives

$$V \partial_\sigma v + \frac{V h^2}{6} L_3[v] = \epsilon (\partial_\sigma^2 v + \partial_\tau^2 v) + \frac{\epsilon h^2}{12} L_4[v] \quad (2.19)$$

with

$$\begin{aligned} L_3[v] &= \frac{1}{4} (3 + \cos(4\theta)) \partial_s^3 v - \frac{3}{4} \sin(4\theta) \partial_s^2 \partial_t v + \frac{3}{2} \sin^2(2\theta) \partial_s \partial_t^2 v + \frac{1}{4} \sin(4\theta) \partial_t^3 v, \\ L_4[v] &= \frac{1}{4} (3 + \cos(4\theta)) (\partial_s^4 v + \partial_t^4 v) - \sin(4\theta) (\partial_s^3 \partial_t v - \partial_s \partial_t^3 v) + 3 \sin^2(2\theta) \partial_s^2 \partial_t^2 v. \end{aligned}$$

Because we are interested in the effects of the internal layer, we expect derivatives of  $v$  in the  $t$ -direction (perpendicular to the layer) to be significantly larger than derivatives in the  $s$ -direction. The scalings (2.10) are selected to balance the terms  $\partial_s v$  and  $\partial_t^2 v$  in (2.19). Thus, upon substituting (2.10) into (2.19) and dropping terms smaller than  $O(\gamma R_h)$ , we obtain

$$\partial_\sigma v = \partial_\tau^2 v - \beta \partial_\tau^3 v + \frac{\gamma}{R_h} \partial_\sigma^2 v + \frac{\gamma R_h}{48} (3 + \cos(4\theta)) \partial_\tau^4 v \quad (2.20)$$

with  $\beta$  as defined by (2.15).

The inexperienced user of modified equations may expect (2.20) to serve as a modified equation for (2.8). We cannot use it because the term involving  $\partial_\tau^4 v$  renders (2.20) unstable to high-frequency perturbations. The use of such a modified equation would predict numerical instabilities where there are none, and it is a disservice to the user of a modified equation not conforming to the difference scheme for phenomena of short wave length. The term  $\partial_\tau^4 v$  appears in (2.20) because we stopped the Taylor expansion (2.18) at  $\partial_\tau^3 v$ , and we went that far because the coefficient  $\beta$  of  $\partial_\tau^3 v$  in (2.20) is zero when  $\sin(4\theta) = 0$ . That is, we must replace  $\partial_\tau^4 v$  by something reasonable but harmless when  $\beta$  is near zero, and for other values of  $\beta$  it need only be something harmless. Because  $\partial_\sigma v \approx \partial_\tau^2 v$  when  $\beta \approx 0$ , the substitution we make to render  $\partial_\tau^4 v$  harmless is that  $\partial_\tau^4 v \approx \partial_\sigma^2 v$ . In this way a high-frequency instability is converted into an increase of dissipation in the streamwise direction, and it produces our modified equation (2.13). (This trick was also used in [13] in the special case  $\theta = 0$ .)

**Remarks to mathematicians.** The above argument contains some sleight of hand. In particular, the domain  $\Omega$  was replaced by the halfspace  $s > 0$  or, equivalently,  $\sigma > 0$ . This change removes any ordinary boundary layer which may be present at the outflow. In addition, boundary data for (2.13) are to be applied at the rotated boundary  $s = 0$ . We expect these distortions to introduce discrepancies only near the point of discontinuity  $(x, y) = (0, y_0)$ . In particular, it appears from our computations that there needs to be a slight shift of coordinates. See the comments concerning Fig. 1 below. We have also not shown that the solution of the modified equation (2.13) bears any resemblance to the solution of the difference scheme (2.8). Such a proof would probably proceed as in [13] with the replacement of  $\Omega$  by the halfspace  $x > 0$ , followed by a Fourier transformation of (2.8) in the  $y$ -direction. The modified equation (2.13) shows that the canonical form of the integral representation of  $v$  is

$$v(\sigma, \tau) = \frac{1}{2} + \int_{-\infty}^{\infty} \frac{f(\omega)}{i2\pi\omega} \exp \{ i a_3 \omega^3 - a_2 \omega^2 + i a_1 \omega \} d\omega \quad (2.21)$$

with  $f$  and the  $a_j$  dependent on  $\sigma$  and  $\tau$ . Furthermore, the integral (2.16) indicates that  $f \approx 1$ ,  $a_3 \approx \beta\sigma$ ,  $a_2 \approx \sigma$ , and  $a_1 \approx \tau$  when  $\sigma \gg 1$  and  $|\tau| \ll 1$ . The integral (2.16) derived from the modified equation (2.14) is merely a nonuniform asymptotic approximation which is valid when  $|\tau| \ll 1$ ,  $\sigma \gg 1$ , and when  $\beta$  is bounded away from zero. We see from the form of (2.21) that a uniform asymptotic estimate would require investigation of the interaction of two saddle points and a pole. For the case when  $\sin(4\theta) = 0$  the situation is simpler because  $a_3 = 0$  and there is only one saddle point and a pole. Uniform asymptotics for  $\theta = 0$  are presented in Hedstrom and Osterheld [13].

**A computational example.** In our computations to illustrate these oscillations we located the point of discontinuity at  $y_0 = 0.25$ , we chose coefficients

$$V \cos \theta = 2, \quad V \sin \theta = 1, \quad \epsilon = 0.002,$$

and we used a mesh size of  $h = 0.02$ . This gives a cell Reynolds number of moderate size  $R_h = 10\sqrt{5}$ , and with  $L = 1$  it gives  $\gamma = 0.02$ . The scaling (2.10) is therefore  $\sqrt{L\epsilon/V} \approx 0.0946$ , and the value of  $\beta$  in (2.15) is  $\beta \approx 0.598$ . The cross section at  $x = 0.8$  is shown in Fig. 1, where the solution to (2.8) is shown as a solid curve and the Airy integral (2.16) is given as dashes. We must admit that in order to obtain such a good match of the curves, we had to shift the jump for the Airy integral from  $y_0$  to  $y_0 + h$ . This could be because the Airy integral applies to the rotated coordinate system  $(s, t)$  given by (2.9). It should also be noted that there is a phase difference between the two curves in the oscillatory region. This is a well-known deficiency of modified equations, and it results from the nonuniformity of the asymptotic approximation. At the point  $(x, y) = (0.8, 0.6)$  near the overshoot the value the parameter  $\alpha$  given by (2.17) is  $\alpha \approx 1.294$ . We have oscillations because  $\alpha < 2$ .

The numerical method we used to solve (2.8) is a combination of ideas from Elman and Golub [9] and from Chin and Manteuffel [6]. As in Elman and Golub, we introduce a red-black ordering on the grid points and do a cyclic reduction to obtain a nine-point scheme on the black grid points. This reduction produces a matrix much better conditioned for iterative methods. The iterative method used by Elman and Golub is point Jacobi, mostly because they impose no constraints on the direction of flow. In our example the flow is one-directional, so we follow Chin and Manteuffel in using line Gauss-Seidel with lines transversal to the flow, starting at the inflow boundary and marching downstream. We find that this scheme converges very rapidly, with the greatest speeds at high cell Reynolds numbers. (Perhaps, we should reiterate that the point of this section is to show that rapid solution of the matrix equation should not be the primary objective-- its solution is a poor approximation to the solution of the differential equation when the parameter  $\beta$  in (2.15) is large.)

Let us remark that we have also solved (2.8) in a version with a discrete approx-

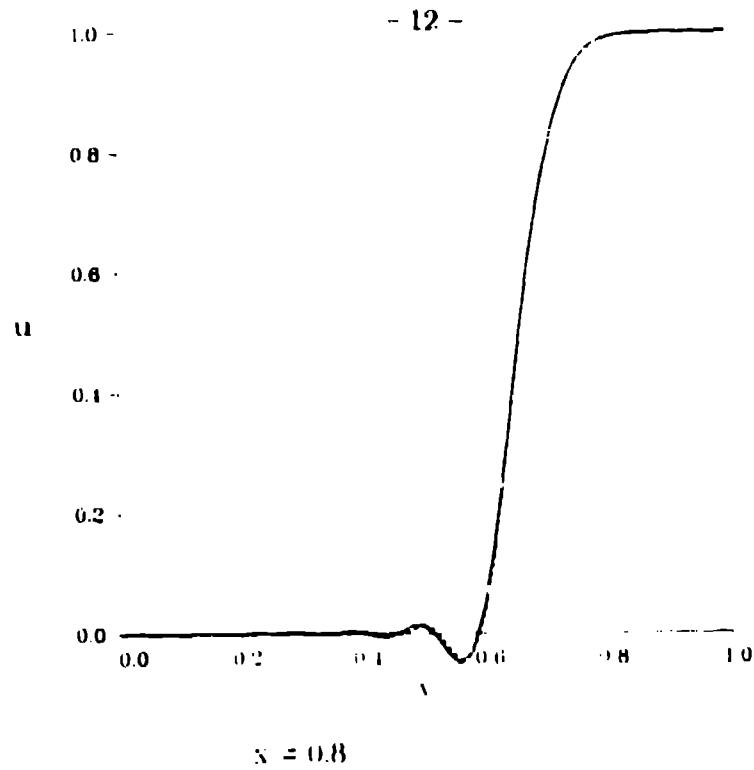


**Fig. 1.** Airy oscillations.

imation to Neumann outflow boundary conditions

$$\begin{aligned} \partial_x u &= 0 \quad \text{for } x = 1, \\ \partial_y u &= 0 \quad \text{for } y = 1. \end{aligned} \tag{2.22}$$

We found this boundary condition to be satisfactory only for small cell Reynolds number,  $R_h < 5$ . Otherwise, there are additional small oscillations with period  $2h$  induced by the mismatch at the outflow boundary  $x = 1$ .

### 3. Curvilinear coordinates.

In this section we permit the coefficients  $a$  and  $b$  in (2.1) to depend on the position  $(x, y)$ , and we present a numerical algorithm for generating an orthogonal coordinate system (a chart) aligned with the given vector field  $(a, b)$ . Our coordinate system is derived from the characteristic curves. We remark that a somewhat different coordinate transformation based on characteristics was given by Chia *et al.* [5].

We again assume that the vector field  $(a, b)$  has no stagnation point, so that  $|a| + |b|$  is bounded away from zero for all  $(x, y)$  in  $\Omega$ . For purposes of constructing the mapping, it is convenient to do an initial scaling so that  $a^2 + b^2 = 1$ . One of our goals is to set up a mapping  $(s, t) \mapsto (x, y)$  such that  $s$  follows the flow in the sense that there exists a positive function  $\phi$  for which

$$\partial_s = \phi(a \partial_x + b \partial_y). \quad (3.1)$$

Because the vector  $(-b, a)$  is orthogonal to  $(a, b)$ , the orthogonality requirement (our second goal) amounts to the condition

$$\partial_t = \psi(-b \partial_x + a \partial_y) \quad (3.2)$$

for some positive function  $\psi$ . In a moment we show that the scale factors  $\phi$  and  $\psi$  are not arbitrary.

In part, the construction of such a mapping is easy, because it is easy to integrate (3.1). All that is needed is to pick a convenient starting point  $(x_0, y_0)$  and to integrate the system

$$\begin{aligned} \frac{dx}{ds} &= a\phi, & x &= x_0 \text{ at } s = 0, \\ \frac{dy}{ds} &= b\phi, & y &= y_0 \text{ at } s = 0. \end{aligned} \quad (3.3)$$

This gives a curvilinear coordinate line in  $\Omega$  corresponding to a constant value of  $t$ . The image of a line  $s = \text{const.}$  may be obtained similarly by integrating

$$\begin{aligned} \frac{dx}{dt} &= -b\psi, & x &= x_0 \text{ at } t = 0, \\ \frac{dy}{dt} &= a\psi, & y &= y_0 \text{ at } t = 0. \end{aligned} \quad (3.4)$$

We still must ensure global consistency as follows. Let us traverse the edges of the curvilinear rectangle  $s_0 < s < s_1$ ,  $t_0 < t < t_1$ , and we assume that this rectangle is contained in  $\Omega$ . Denote the image of  $(s_0, t_0)$  as the vertex  $A$ . Suppose further that we integrate (3.3) from  $s_0$  to  $s_1$ , arriving at the vertex  $C$ . We then integrate (3.4) from  $t_0$  to  $t_1$  and arrive at the vertex  $B$  opposite  $A$ . Let us now reverse the order by first integrating (3.4) from  $t_0$  to  $t_1$  to arrive at the vertex  $D$  and then integrate (3.3)

from  $s_0$  to  $s_1$ . Can we be certain that we again arrive at the vertex B? It happens that this global consistency question has been answered [15], and that what is required is the vanishing of the Lie bracket  $[\partial_s, \partial_t] = \partial_s \partial_t - \partial_t \partial_s$ .

It is easy to see by a short computation that the vanishing of the Lie bracket  $[\partial_s, \partial_t]$  is equivalent to the system of partial differential equations

$$\begin{aligned}\partial_s(a\psi) &= \partial_t(b\phi), \\ \partial_s(b\psi) &= -\partial_t(a\phi).\end{aligned}\tag{3.5}$$

Upon differentiating the product in (3.5) and solving for  $\partial_s\psi$  and  $\partial_t\phi$ , we find that a necessary and sufficient condition for consistency is that

$$\begin{aligned}(a^2 + b^2) \partial_s\psi &= \phi(a \partial_t b - b \partial_t a) - \psi(a \partial_s a + b \partial_s b), \\ (a^2 + b^2) \partial_t\phi &= -\phi(a \partial_t a + b \partial_t b) + \psi(b \partial_s a - a \partial_s b).\end{aligned}\tag{3.6}$$

Note that if  $(a, b)$  has been scaled so that  $a^2 + b^2 = 1$ , then (3.6) takes the simpler form.

$$\begin{aligned}\partial_s\psi &= \phi(a \partial_t b - b \partial_t a), \\ \partial_t\phi &= \psi(b \partial_s a - a \partial_s b).\end{aligned}\tag{3.7}$$

We recognize the system (3.7) as the telegraphers' equation, written in terms of Lie derivatives along the characteristic curves. Therefore, all that is needed for its solution is to prescribe values  $\phi = 1$  at  $t = 0$  and  $\psi = 1$  at  $s = 0$  and to march in the  $s$  and  $t$ -directions concurrently.

It should be emphasized that theoretical questions remain for this grid-generation scheme. In particular, there is no guarantee that the solutions  $\phi$  and  $\psi$  will be positive at all points in  $\Omega$ . This is important in that the Jacobian of the transformation (3.3-4) is given by  $J = (a^2 + b^2)\phi\psi$ . We required at the outset that  $a^2 + b^2$  be bounded away from zero. Thus, if we are to maintain a nonzero Jacobian, we must take special measures whenever it happens that  $\phi \leq 0$  or  $\psi \leq 0$ . One possibility is to back up and put a boundary on this local chart. We could then initialize a new chart and continue.

#### 4. Domain decomposition for an internal layer.

In this section we present a computational example which uses domain decomposition to resolve an internal layer. At this point we have not yet implemented the algorithm described here, but the final report will have computations. In our algorithm we first identify the internal and boundary layers, and we then set up a domain decomposition to segregate them. The domain decomposition is carried out with overlapping using the tools of Chesshire and Henshaw [2]. We have added the modification that in some subdomains we use the grid-generation algorithm of Section 3.

As our domain  $\Omega$  we use the square  $0 < x < 1$ ,  $0 < y < 1$ , and on  $\Omega$  we consider the convection-diffusion equation

$$(1+x)\partial_x u + (1-y)\partial_y u = \epsilon \Delta u.$$

As boundary conditions for (4.1) we prescribe  $u = 0$  on the bottom of  $\Omega$ ,  $u = 1$  on the left-hand edge ( $x = 0$ ),  $u = 1$  on the top ( $y = 1$ ), and  $u = 0$  on the right-hand edge ( $x = 1$ ).

Note that in (4.1) we have chosen coefficients so that there is no turning point in  $\Omega$ . That is, we have  $|1+x| + |1-y|$  bounded away from zero in  $\Omega$ . Note also that by the discussion in Section 1 the inflow boundary  $\Gamma_I$  consists of the bottom  $y = 0$  and the left-hand side  $x = 0$  of the square  $\Omega$ . Furthermore, the top of the square  $y = 1$  is a tangential boundary  $\Gamma_T$ , and the right-hand edge  $x = 1$  is an outflow  $\Gamma_O$ . The reduced equation is

$$(1+x)\partial_x U + (1-y)\partial_y U = 0, \quad (4.2)$$

and its boundary conditions are imposed on the inflow boundary  $\Gamma_I$ . It so happens that we can write down a formula for the solution  $U$  of (4.2), although it is not necessary for our domain-decomposition algorithm. The characteristic curves for (4.2) are the hyperbolas  $(x-1)(y+1) = \text{const.}$  Thus, the solution of the reduced equation (4.2) is

$$U = \begin{cases} 1 & \text{if } y > x/(x+1), \\ 0 & \text{if } y < x/(x+1). \end{cases}$$

This gives us an internal layer along the hyperbola  $y = x/(x+1)$  and exponential boundary layers at the outflow boundary  $x = 1$ . It happens that we imposed boundary data along the tangential boundary  $\Gamma_T$  such that no boundary layer resides there. If there had been a boundary layer along  $\Gamma_T$ , we could have modified the domain decomposition described below so as to include its effects.

As the problem is stated, we need the following subdomains: (1) a square  $B$  of diameter  $O(\epsilon)$  at the origin to cover the birth of the internal layer, (2) an internal layer region

$$I = \{(x, y): |y - x/(x+1)| \leq C\sqrt{\epsilon x}\}$$



with  $O(\epsilon) < x < 1 - O(\epsilon)$ , (3) three outflow boundary layers  $\mathcal{O}$ , one above the internal layer, one below it, and one interacting with it, (4) an outer region  $\mathcal{H}$  above the internal layer on which  $u \approx 1$ , and (5) an outer region  $\mathcal{H}$  below the internal layer on which  $u \approx 0$ .

In the two outer regions  $\mathcal{H}$  we use a coordinate system derived from the characteristics, as described in Section 3. In the internal layer  $\mathcal{I}$  we use a parabolic coordinate system imposed on the characteristics. (More precise details will be given in the final report.) Finally, in the birth  $\mathcal{B}$  and boundary-layer regions  $\mathcal{O}$  we use the methods given in the papers by Hedstrom and Howes [11] and [12]. The iterations are performed in the order: (1) the outer regions  $\mathcal{H}$ , (2) the birth region  $\mathcal{B}$ , (3) the internal layer  $\mathcal{I}$ , (4) the outflow boundary layers  $\mathcal{O}$ . The iterative schemes in the subdomains are as in [10] and [12].

**Acknowledgments.** The work of the first author (D. L. B.) was supported by Los Alamos National Laboratory through the U. S. Department of Energy under contract W-7405-ENG-36. The work of the second and third authors (R. C. Y. C. and G. W. H.) was supported by the Applied Mathematical Sciences subprogram of the Office of Energy Research, U. S. Department of Energy by the Lawrence Livermore National Laboratory under contract number W-7405-ENG-48.

## References

- [1] K. W. Chang and F. A. Howes, *Nonlinear Singular Perturbation Phenomena: Theory and Applications*, Springer-Verlag, New York, 1984.
- [2] G. Chesshire and W. D. Henshaw, 'Composite overlapping meshes for the solution of partial differential equations', *J. Comput. Phys.* **90** (1990), 1-64.
- [3] R. C. Y. Chin and G. W. Hedstrom, 'A dispersion analysis for difference schemes: Tables of generalized Airy functions', *Math. Comput.* **32** (1978), 1163-1170.
- [4] R. C. Y. Chin and G. W. Hedstrom, 'Domain decomposition: An instrument of asymptotic-numerical methods', to appear in the Proceedings of the Workshop on Asymptotics and Numerics, H. Kaper, ed., Marcel Dekker.
- [5] R. C. Y. Chin, G. W. Hedstrom, F. A. Howes, and J. R. McGraw, 'Parallel computation of multiple-scale problem', pp. 136-154 in *New Computing Environments: Parallel, Vector and Systolic*, A. Wouk, ed., Society for Industrial and Applied Mathematics, Philadelphia, 1986.
- [6] R. C. Y. Chin and T. A. Manteuffel, 'An analysis of block successive overrelaxation for a class of matrices with complex spectra', *SIAM J. Numer. Anal.* **25** (1988), 564-585.
- [7] P. Colella and P. R. Woodward, 'The piecewise parabolic method for gas dynamic simulations', *J. Comput. Phys.* **54** (1984), 174-201.

- [8] W. Eckhaus, *Asymptotic Analysis of Singular Perturbations*, North-Holland, Amsterdam, 1979.
- [9] H. C. Elman and G. H. Golub, 'Iterative methods for cyclically reduced non-self-adjoint linear systems', *Math. Comp.* **54** (1990), 671-700.
- [10] D. F. Griffiths and J. M. Sanz-Serna, 'On the scope of the method of modified equations', *SIAM J. Sci. Stat. Comput.* **7** (1986), 994-1008.
- [11] G. W. Hedstrom and F. A. Howes, 'A domain decomposition method for a convection diffusion equation with turning point', pp. 38-46 in *Domain Decomposition Methods*, T. F. Chan, R. Glowinski, J. Periaux, and O. B. Widlund, eds., Society for Industrial and Applied Mathematics, Philadelphia, 1989.
- [12] G. W. Hedstrom and F. A. Howes, 'Domain decomposition for a boundary-value problem with a shock layer', pp. 130-140 in *Domain Decomposition Methods for Partial Differential Equations*, T. F. Chan, R. Glowinski, J. Periaux, and O. B. Widlund, eds., Society for Industrial and Applied Mathematics, Philadelphia, 1990.
- [13] G. W. Hedstrom and A. Osterheld, 'The effect of cell Reynolds number on the computation of a boundary layer', *J. Comput. Phys.*, **37** (1980), 399-421.
- [14] P. L. Roe, 'Discrete models for the numerical analysis of time dependent multi-dimensional gas dynamics', *J. Comput. Phys.* **63** (1986), 458-476.
- [15] M. Spivak, *Differential Geometry*, vol. 1, second ed., Publish or Perish, Houston, 1979.
- [16] R. F. Warming and B. J. Hyett, 'The modified equation approach to the stability and accuracy of finite-difference methods', *J. Comput. Phys.* **14** (1974), 159-179.